

Bone marrow progenitor cells do not contribute to liver fibrogenic cells

Bruno Diaz Paredes, Lanuza Alaby Pinheiro Faccioli, Luiz Fernando Quintanilha, Karina Dutra Asensi, Camila Zaverucha do Valle, Paulo César Canary, Christina Maeda Takiya, Antonio Carlos Campos de Carvalho, Regina Coeli dos Santos Goldenberg

Bruno Diaz Paredes, Lanuza Alaby Pinheiro Faccioli, Luiz Fernando Quintanilha, Karina Dutra Asensi, Camila Zaverucha do Valle, Christina Maeda Takiya, Antonio Carlos Campos de Carvalho, Regina Coeli dos Santos Goldenberg, Carlos Chagas Filho Biophysics Institute, Rio de Janeiro 21941-902, Brazil

Paulo César Canary, Radiology Department, Clementino Fraga Filho University Hospital, Rio de Janeiro 22909-538, Brazil

Author contributions: Paredes BD and Faccioli LAP contributed equally to this work and participated in the experimental design, performed flow cytometry, fluorescence assays, and analyzed the data; Quintanilha LF performed mouse liver injury and data analysis; Asensi KD performed bone marrow transplantation and data analysis; Zaverucha-do-Valle C performed confocal microscopy and data analysis; Canary PC performed mouse whole-body irradiation and data analysis; Takiya CM performed histology and data analysis; Campos-de-Carvalho AC participated in the experimental design and statistical analysis; Goldenberg RCS designed and supervised the study, execution, analysis and approved the final version; and all authors participated in manuscript preparation.

Supported by Brazilian Council for Scientific and Technological Development; Coordination for the Improvement of Higher Education Personnel; Rio de Janeiro State Research Supporting Foundation and Ministry of Health

Correspondence to: Regina Coeli dos Santos Goldenberg, PhD, Carlos Chagas Filho Biophysics Institute, Carlos Chagas Filho Avenue, 373, Health Sciences Center, Corridor G, 2nd floor/room 53-University City, Rio de Janeiro 21941-902, Brazil. rcoeli@biof.ufrj.br

Telephone: +55-21-25626559 Fax: +55-21-25626559

Received: December 6, 2011 Revised: October 24, 2012

Accepted: October 26, 2012

Published online: October 27, 2012

Abstract

AIM: To investigate the contribution of bone marrow (BM) cells to hepatic fibrosis.

METHODS: To establish a model of chimerism, C57Bl/6 female mice were subjected to full-body irradiation (7 Gy) resulting in BM myeloablation. BM mononuclear cells obtained from male transgenic mice expressing enhanced green fluorescent protein (GFP) were used for reconstitution. Engraftment was confirmed by flow cytometry. To induce liver injury, chimeric animals received carbon tetrachloride (CCl₄) 0.5 mL/kg intraperitoneally twice a week for 30 d (CCl₄ 30 d) and age-matched controls received saline (Saline 30 d). At the end of this period, animals were sacrificed for post mortem analysis. Liver samples were stained with hematoxylin and eosin to observe liver architectural changes and with Sirius red for collagen quantification by morphometric analysis. α -smooth muscle actin (α -SMA) was analyzed by confocal microscopy to identify GFP+ cells with myofibroblast (MF) characteristics. Liver tissue, BM and peripheral blood were collected and prepared for flow cytometric analysis using specific markers for detection of hepatic stellate cells (HSCs) and precursors from the BM.

RESULTS: Injury to the liver induced changes in the hepatic parenchymal architecture, as reflected by the presence of inflammatory infiltrate and an increase in collagen deposition (Saline 30 d = 11.10% \pm 1.12% vs CCl₄ 30 d = 12.60% \pm 0.73%, P = 0.0329). Confocal microscopy revealed increased reactivity against α -SMA in CCl₄ 30 d compared to Saline 30 d, but there was no co-localization with GFP+ cells, suggesting that cells from BM do not differentiate to MFs. Liver flow cytometric analysis showed a significant increase of CD45+/GFP+ cells in liver tissue (Saline 30 d = 3.2% \pm 2.2% vs CCl₄ 30 d = 5.8% \pm 1.3%, P = 0.0458), suggesting that this increase was due to inflammatory cell infiltration (neutrophils and monocytes). There was also a significant increase of common myeloid progenitor cells (CD117+/CD45+) in the livers of CCl₄-treated animals

(Saline 30 d = 2.16% ± 1.80% vs CCl₄ 30 d = 5.60% ± 1.30%, *P* = 0.0142). In addition the GFP-/CD38+/CD45- subpopulation was significantly increased in the CCl₄ 30 d group compared to the Saline 30 d group (17.5% ± 3.9% vs 9.3% ± 2.4%, *P* = 0.004), indicating that the increase in the activated HSC subpopulation was not of BM origin.

CONCLUSION: BM progenitor cells do not contribute to fibrosis, but there is a high recruitment of inflammatory cells that stimulates HSCs and MFs of liver origin.

© 2012 Baishideng. All rights reserved.

Key words: Bone marrow; Liver; Fibrosis; Progenitor cells; Chimeric mice; Green fluorescent protein+ cells

Peer reviewers: Guangcun Huang, MD, PhD, Center for Clinical and Translational Research, the Research Institute at Nationwide Children's Hospital, Columbus, OH 43205, United States; Waka Ohishi, Department of Clinical Studies, Radiation Effects Research Foundation, Hiroshima 732-0815, Japan

Paredes BD, Faccioli LAP, Quintanilha LF, Asensi KD, Zaverucha-do-Valle C, Canary PC, Takiya CM, Campos-de-Carvalho AC, Goldenberg RCS. Bone marrow progenitor cells do not contribute to liver fibrogenic cells. *World J Hepatol* 2012; 4(10): 274-283 Available from: URL: <http://www.wjgnet.com/1948-5182/full/v4/i10/274.htm> DOI: <http://dx.doi.org/10.4254/wjh.v4.i10.274>

INTRODUCTION

In recent years, cell transplantation has emerged as a potential therapy to improve impaired liver function. In particular, bone marrow-derived stem cells (BMSCs) have been widely used in pre-clinical and clinical trials^[1].

Interest in this particular cell type was kindled by the discovery of donor-derived cells in the livers of bone marrow (BM) transplant recipients^[2]. This indicated a potential relationship between BM and the regenerating liver. However, results published so far show no consensus as to the role of BMSCs in liver repair, and the issue remains one of the most controversial in regenerative medicine.

Several studies using different experimental models of hepatic diseases have demonstrated functional recovery of the liver after cell therapy^[3-6]. On the other hand, our group, in agreement with the results of several other studies^[7-9], did not observe any benefits of using the bone marrow mononuclear cell fraction from normal^[10] or cirrhotic rats^[11] or BM-derived stromal cells^[12] in a severe chronic hepatic injury model in rats.

Hepatic fibrosis and cirrhosis are the main causes of organ failure in chronic liver diseases of any etiology^[13]. Persistent parenchymal cell injury leads to dysregulation of the normal processes of wound healing and to extensive deposition of extracellular matrix proteins^[14], a dynamic process known as fibrogenesis. This pathol-

ogy involves various cellular and molecular mechanisms, in which the myofibroblast (MF) and hepatic stellate cell (HSC) subpopulations play a major role when they become activated^[15].

During fibrogenesis, activated HSCs, located mainly in the perisinusoidal space, go through a transdifferentiation process, changing to a MF-like morphology at the portal spaces^[16]. MFs present at these sites display high rates of proliferation, excessive production of collagen fibers and decreased production of matrix metalloproteinases, causing an imbalance in matrix degradation and preventing the resolution of fibrosis^[17]. Both the MF and activated HSC subpopulations express α -smooth muscle actin (α -SMA), a known marker of pro-fibrotic cells^[18].

BMSCs may also play a role in generating liver fibrosis. Many authors reported that fibrocytes^[19], a BM-derived CD45+/CD34+/procollagen type 1+ subpopulation, can contribute to fibrosis in different models such as chronic cystitis^[20], ischemic cardiomyopathy^[21] and asthma^[22]. In addition, in a rat biliary duct ligation liver injury model, BM-derived fibrocytes [expressing collagen α 1(I) promoter-green fluorescent protein (GFP)] were reported to comprise 5% of all collagen-producing cells^[23], an impressive percentage considering the low frequency of this cell type under normal conditions (0.1%-1.0% in humans)^[24].

In this scenario, where the use BM-derived cell therapies in liver disease is still controversial, it is important to investigate whether BM-derived cells can in fact contribute to liver fibrosis.

MATERIALS AND METHODS

Animals

All procedures were performed in accordance with the standards of the Guide for Care and Use of Laboratory Animals (DHHS Publication No. NIH 85-23, revised 1996, Office of Science and Health Reports, Bethesda, MD 20892). Female C57/BL6 mice and male mice transgenic for GFP- line C57/BL6-Tg (CAG-EGFP) C14-Y01-FM1310 (GFP+ mice), donated by Okabe *et al.*^[25], were obtained from the Carlos Chagas Filho Institute of Biophysics animal facility. Animals were housed at a controlled temperature (23 °C) and 12-h light-dark cycle.

Experimental model: Total body irradiation and cell transplants

Female mice 6-8 wk of age were exposed to whole-body radiation (7 Gy) in a linear accelerator (Varian-Clinac 2100 CD) used for radiotherapy. BM cells were harvested from the femurs and tibiae of 8- to 12-wk-old male mice expressing enhanced GFP. Bones were inserted into adapted centrifuge tubes and centrifuged for 3 min at 1500 × *g* to collect the marrow. The contents were resuspended in Dulbecco's Modified Eagle's Medium (DMEM-Invitrogen) and layered on Histopaque 1083 (Sigma). The tubes were centrifuged at 400 × *g* for 30 min and the band corresponding to mononuclear cells

Table 1 Antibody panel for flow cytometric analysis of specific cells

Tubes	Cell number	Antibodies	Dil.	Target cells (tissue)
Control	1 × 10 ⁵	No antibodies	-	-
1	1 × 10 ⁶	CD45-PE-Cy7 (BD Biosciences)	1:25	Hepatic stellate cells (liver)
		CD38-PE-Cy5 (eBioscience)	1:10	
2	1 × 10 ⁶	CD45-PE-Cy7 (BD Biosciences)	1:25	Hematopoietic stem cells, fibrocytes and monocytes (BM, PB and liver)
		CD14-APC (eBioscience)	1:10	
		CD34-PE (eBioscience)	1:10	
3	1 × 10 ⁶	CD45-PE-Cy7 (BD Biosciences)	1:25	Hematopoietic stem cells, fibrocytes and endothelial progenitor Cells (BM, PB and liver)
		CD133-APC (eBioscience)	1:10	
		CD34-PE (eBioscience)	1:10	
4	1 × 10 ⁶	CD45-PE-Cy7 (BD Biosciences)	1:25	Common progenitor cells (BM)
		CD117-APC (eBioscience)	1:10	
		CD34-PE (eBioscience)	1:10	

BM: Bone marrow; PB: Peripheral blood.

was collected. The cells were then washed and counted and their viability determined by Trypan blue exclusion. The mononuclear cells were resuspended in sterile saline (NaCl 0.9%) and injected through the orbital plexus in the female wild-type (WT) previously irradiated mice.

Experimental groups

Infused animals were maintained under observation for 21 d after transplantation. Then, peripheral blood (PB) samples were collected to verify transplant efficiency by flow cytometric analysis of GFP+ cells. Animals showing percentages above 80% GFP+ cells were considered useful chimeric mice. PB samples of WT C57/BL6 and GFP+ mice were used as negative and positive controls, respectively. Selected chimeric mice ($n = 10$) were divided into two groups: CCl₄ 30 d ($n = 5$), which received injections of carbon tetrachloride (CCl₄; dose of 0.5 mL/kg) twice a week for 30 d, and Saline 30 d ($n = 5$) (experimental control), which received injections of saline solution during the same period.

Histology

Liver tissue slices were fixed for 5 h in Gendre's solution, then overnight in 10% buffered formalin solution (pH 7.2) and embedded in paraffin. Liver samples were sectioned (5 μm) and stained with hematoxylin-eosin (HE) and Sirius red. According to standard protocols, histomorphometry was performed using an imaging system consisting of a Q-Color 5 digital camera (Olympus, Japan) coupled to an epifluorescence Axiovert 100 microscope (Carl Zeiss, Thornwood, NY, United States). Randomly picked fields of Sirius red sections were captured from each animal, using a 20 × objective lens. Quantification was estimated by the percentage of stained area in comparison to the total area of the fields examined, using Image-Pro Plus 5.0 (Media Cybernetics, Bethesda, MD, United States) image analysis software.

Peripheral blood samples for flow cytometry analysis

First, 50 μL of PB samples from tail veins of irradiated animals were collected at day 21 to evaluate GFP+

BM engraftment efficiency. WT and GFP+ PB samples were used as negative and positive controls, respectively. Erythrocyte lysis-fixation solution (BD FACS Lysing Solution, Becton Dickinson) was added to the samples as recommended by the manufacturer and incubated for 15 min at room temperature. After this period, samples were washed with phosphate-buffered saline (PBS) and centrifuged at 300 × *g* for 3 min and resuspended in 300 μL of PBS for data acquisition by flow cytometry (BD FACSAria, Becton Dickinson).

After the injury induction protocol, 0.3 mL of blood was drawn from the tail veins of animals from the experimental and control groups. Samples and antibodies were prepared as described in Table 1 and incubated 20 min in the dark at 4 °C.

Digested liver tissue for flow cytometry analysis

The left hepatic lobe was carefully harvested and mechanically and enzymatically digested with type II collagenase (Worthington) solution 0.2% at 37 °C. After centrifugation at 250 × *g*, the pellet was suspended in 1 mL PBS-bovine serum albumin (BSA) 1% solution and filtered through 30 μm nylon filters (Filcons, Consults). The liver cells obtained were then resuspended in 300 μL PBS-BSA 1% and incubated in the dark for 20 min at 4 °C with anti CD45-PE-Cy7 (BD Biosciences, San Jose, CA), anti CD38-PE-Cy5, anti CD34-PE, anti CD133-APC (all from eBioscience, San Diego, CA) for analysis by flow cytometry. After antibody incubation, stained liver cells were washed twice with PBS by centrifugation at 300 × *g* and 300 μL of PBS was added to prepare the cell suspension. All assays were conducted using concentrations of antibodies recommended by the manufacturers.

All data were obtained using a BD FACSAria II flow cytometer (BD Biosciences) and BD FACSDiva acquisition software (version 6). The exported FCS 3.0 data file was analyzed using FlowJo version 7.6.4.

Direct fluorescence

Liver samples were embedded in Optimal Cutting Tem-

perature (OCT) compound (Tissue-Tek., Sakura, Japan) and preserved at -70 °C. Sections (6 µm) were obtained using a cryostat (Leica CM1850, Leica) at -20 °C and fixed in acetone at 4 °C. Sections were incubated for 5 min in 5 µL of 4, 6-diamino-2-phenylindole (1 mg/mL) and 5 µL of an antifading medium (VectaShield, Vector Laboratories).

Fluorescence was observed on a Zeiss LSM 510 Meta confocal microscope (Carl Zeiss, Thornwood, NY, United States). The specificity of the immunofluorescent staining was assessed for each experimental condition by performing the reaction in the absence of primary antibodies. No staining was observed under such conditions.

Immunofluorescence

Liver tissue was embedded in OCT (Tissue-Tek., Sakura, Japan) and preserved at -70 °C. Sections (6 µm) were obtained using a cryostat (Leica CM 1850, Leica) at -20 °C and fixed in acetone at 4 °C. Subsequently, sections were incubated in blocking solution (5% normal goat serum, 5% BSA in PBS, 0.1% Triton X-100, 0.05% Tween 20, 0.01% gelatin, all from Sigma Chemical Co.) for 1 h. Endogenous biotin was inhibited by using streptavidin and biotin solutions from a Dako blocking kit (Dako) according to the manufacturer's instructions. Indirect immunofluorescence technique was used to detect activated HSCs and MFs, using a primary monoclonal anti- α -SMA antibody (Dako, dilution of 1:40) biotinylated with the Animal Research Kit. Sections were incubated overnight at 4 °C and then washed twice in PBS-Tween 0.25% and then, the sections were incubated for 1.5 h with a streptavidin-Alexa 586 (Molecular Probes, Eugene, OR, United States) and the dye TO-PRO 3, at 1 mmol/L in DMSO (Invitrogen). After two washes in PBS-Tween 0.25% for 10 min, sections were mounted with Vectashield. Anti-mouse IgG was used as an isotype control. Serial plane images of 1.0 mm thick sections were obtained using a Zeiss LSM 510 Meta laser scanning confocal microscope (Carl Zeiss, Thornwood, NY, United States).

Statistical analysis

Data were analyzed using analysis of variance (ANOVA) with Dunnett's post-test for multiple comparisons and the *t* test when comparing two groups. $P < 0.05$ was considered statistically significant. The data are presented as mean \pm SD (for Dunnett) and median and 25%-75% percentile (for Mann-Whitney post-test). GraphPad Prism 5 software was used.

RESULTS

Abnormal histological findings are only present in livers of irradiated and CCl₄-intoxicated animals

Initially, HE and Sirius Red staining were performed to evaluate whether the radiation procedure used for BM ablation could induce hepatic lesions. Pre-experimental observations showed that livers from irradiated animals presented no histological changes, displaying regular he-

patic architecture and no septa formation, as observed in non-irradiated WT. The same characteristics were observed in animals from the Saline 30 d group (Figure 1A and C).

After 30 d of intoxication, livers from the CCl₄ 30 d group showed inflammatory infiltration in regions of the centrilobular and portal veins (Figure 1B), indicating hepatocellular damage. Also, the CCl₄ 30 d group showed formation of initial thin septae originating from regions around the centrilobular veins (Figure 1D), indicating deposits of collagen replacing parenchymal cells (fibrosis). Morphometric analysis indicated a significant increase ($P = 0.0329$) in collagen content in CCl₄ 30 d group animals compared to Saline 30 d group animals (Figure 2).

Analysis of GFP+ cells derived from bone marrow in peripheral blood of irradiated/CCl₄-intoxicated animals

Blood population analysis showed that samples from all chimeric animals contained a mean of 88% CD45+/GFP+ cells, while 12% were CD45+/GFP-. Among the CD45+/GFP+ population, there was a significant decrease in total lymphocytes and a significant increase in monocytes and neutrophils (Figure 3).

We also analyzed the presence of GFP+ BM-derived precursor cells in the blood, analyzing hematopoietic precursor cells (CD45+/CD34+) (Figure 4A) and endothelial precursor cells (CD45+/CD133+) (Figure 4B). There was no significant difference in these precursor cells between the Saline 30 d and CCl₄ 30 d groups (Figure 4C and D).

CD117 (c-Kit) precursor cells were analyzed in the BM (Figure 5A). The findings show a significant increase ($P = 0.0142$) in CD45+/GFP+/CD117+ cells in the CCl₄ 30 d group (5.2% \pm 1.3%) compared to the Saline 30 d group (2.6% \pm 1.8%) (Figure 5B).

Bone marrow-derived cells are present in liver tissue

We analyzed cells from digested liver tissue and observed four well-defined subpopulations (Figure 6A): (1) high frequencies of GFP+/CD45+ and GFP-/CD45+ and (2) low frequencies of GFP+/CD45- and GFP-/CD45-. To identify cells of BM origin in liver tissue, we analyzed the GFP+/CD45+ subpopulation and observed a significant increase in this subpopulation in intoxicated livers (Saline 30 d = 3.2% \pm 2.2% vs CCl₄ 30 d = 5.8% \pm 1.3%; $P = 0.0458$) (Figure 6B).

To identify HSCs, we used the CD38 surface marker. This molecule is known to identify B lymphocytes and activated T cells and also labels HSCs^[26], indicating their presence in liver tissue. We identified two subpopulations of CD38+ cells: GFP+/CD38+ and GFP-/CD38+ (Figure 7A). We analyzed the GFP-/CD38+ subpopulation and found two other subpopulations: CD45+ and CD45- (Figure 7B). We also found that the GFP+/CD38+ cells were 100% CD45+ (Figure 7C). Considering that HSCs do not express the CD45 marker, we evaluated the GFP-/CD38+/CD45- subpopulation. We found a significant increase in that subpopulation when

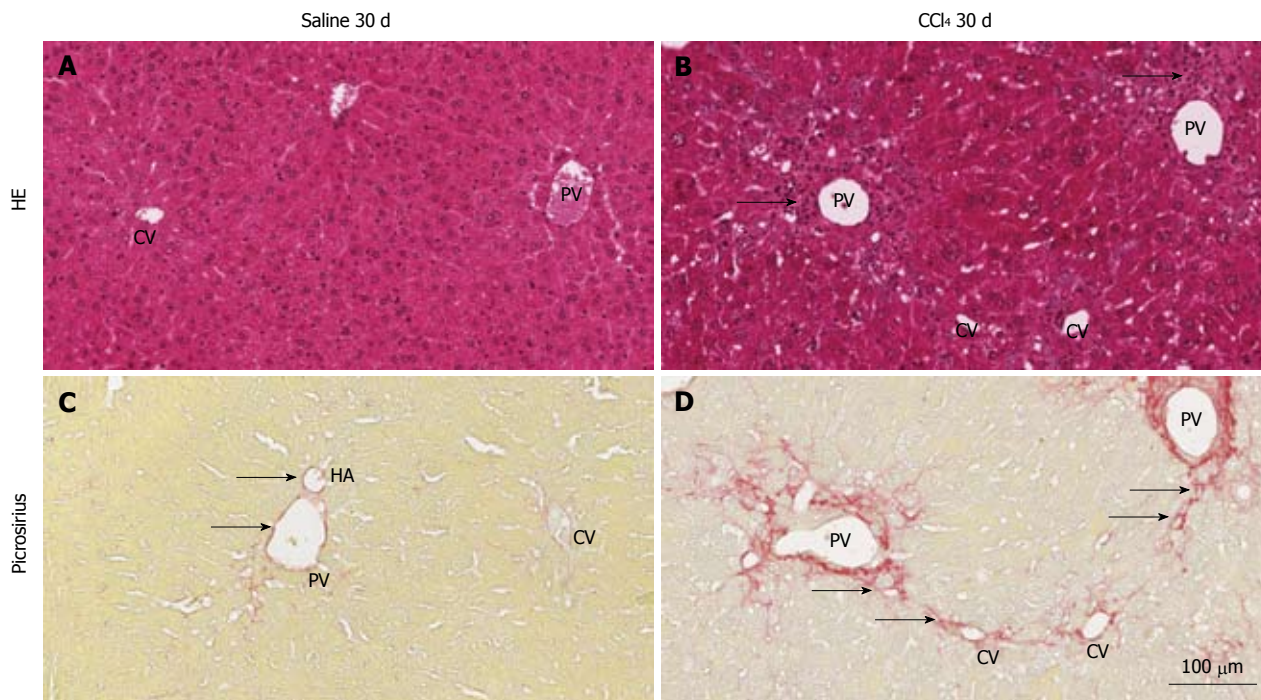


Figure 1 Representative images of histological sections of livers of normal and chimeric animals stained with hematoxylin and eosin or picrosirius. A: hematoxylin and eosin (HE): shows the central vein (CV), portal vein (PV) and regular hepatocyte plates, representing normal architecture of the liver; B: The PV and CV present inflammatory infiltrate (arrows) due to injury of hepatocytes in this region by CCl₄; C: Picrosirius: collagen (red) is present only in the perivascular region of the PV, hepatic artery (HA) (arrows) and lightly present surrounding the VC; D: a high deposition of collagen surrounding the PV and radiating fibers to the CV, indicating initiation of collagen septa (arrows) formation 30 d after injury induction.

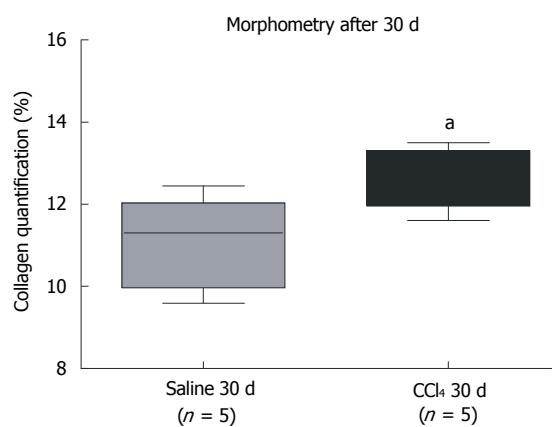


Figure 2 Quantification of collagen by morphometric analysis. A significant increase in collagen between the group that received CCl₄ compared to the group that received saline. The groups are represented by box-whisker diagrams in which the values in the boxes represent the medians of collagen content (n = 5) and the bars the 25%-75% range. The Mann-Whitney post-test was used to test for significance. ^aP = 0.0329 vs the Saline 30 d group.

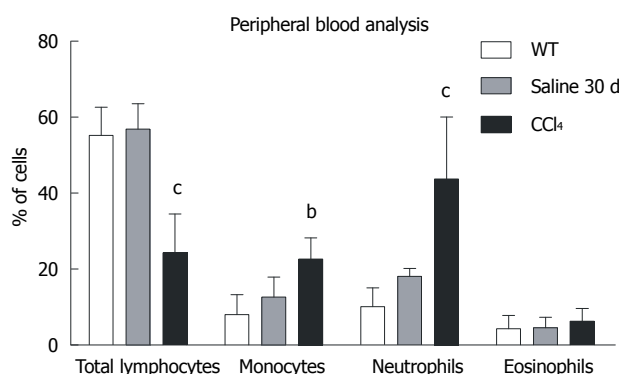


Figure 3 Graphical analysis of subpopulations of peripheral blood of the WT, Saline 30 d and CCl₄ 30 d groups by flow cytometry. Only the animals in CCl₄ 30 d group showed significant differences from wild-type (WT): Total lymphocytes (WT = 55.2% ± 7.4%; Saline 30 d = 56.9% ± 6.6%; CCl₄ 30 d = 24.3% ± 10.2%); Monocytes (WT = 8.1% ± 5.3%; Saline 30 d = 12.7% ± 5.3%; CCl₄ 30 d = 22.7% ± 5.6%); Neutrophils (WT = 10.1% ± 5.0%; Saline 30 d = 18.2% ± 2.1%; CCl₄ 30 d = 43.8% ± 16.3%). One-way analysis of variance (ANOVA) followed by Dunnett's test for multiple comparisons was used. ^bP < 0.01, ^cP < 0.001 vs WT.

comparing the Saline 30 d group (9.3% ± 2.4%) to the CCl₄ 30 d (17.5% ± 3.9%) group (P = 0.004) (Figure 7D), indicating that the increase in the HSC subpopulation was not of BM origin. We did not observe a significant increase in the GFP⁺/CD38⁺/CD45⁺ population between the experimental groups, suggesting that there is no increase in B and T mobilization after injury (data not shown).

No evidence of bone marrow contribution to liver fibrogenesis

The Saline 30 d group showed fusiform cells with green fluorescence, most of them situated in the sinusoidal space and a few in perivascular regions (Figure 8A), as found in GFP⁺ animals (data not shown). In contrast, the CCl₄ 30 d group showed a higher number of GFP⁺ cells diffusely distributed in the parenchyma and perivas-

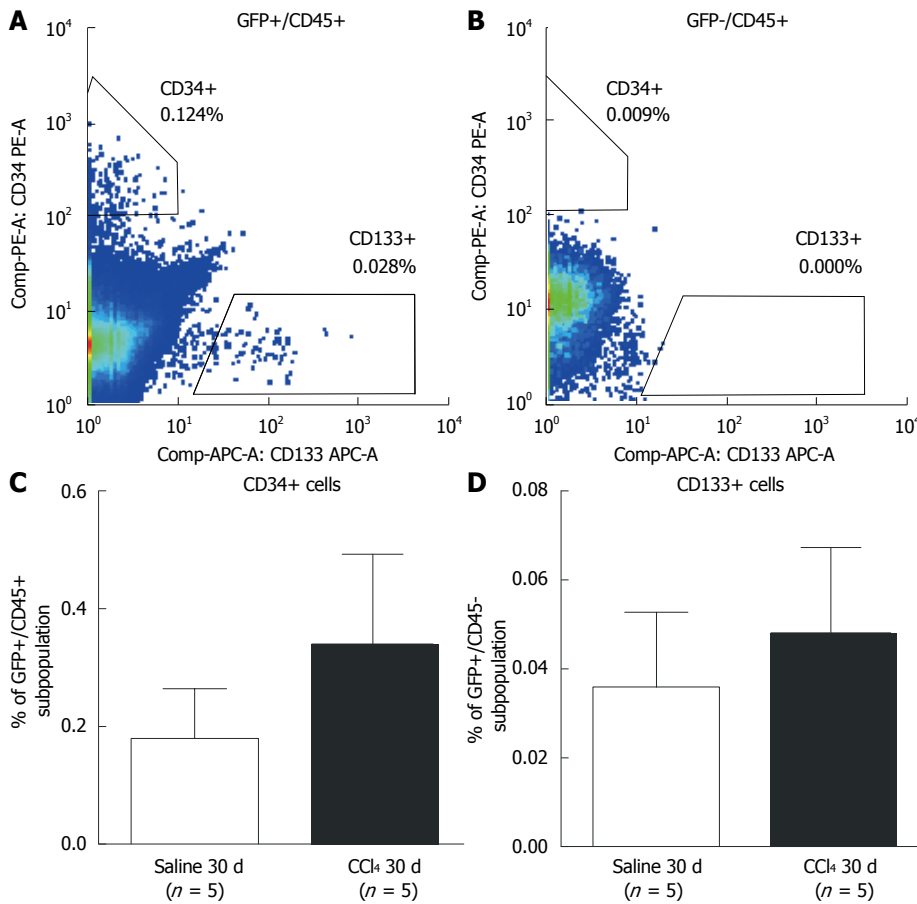


Figure 4 Flow cytometric analysis of subpopulations of hematopoietic and endothelial progenitor cells in bone marrow of chimeric mice. A: Representative results showing green fluorescent protein (GFP)+ precursor cells in both the Saline 30 d and CCl₄ 30 d groups (side bar = ancestry gating). CD45+/CD34+ (hematopoietic) and CD45+/CD133+ (endothelial) cells were identified; B: Representative results showing GFP-subpopulation precursor cells in the Saline 30 d and CCl₄ 30 d groups (side bar = ancestry gating). No progenitor cells were found in the GFP-subpopulation; C: Graphic of the percentage of GFP+/CD45+/CD34+ cells (hematopoietic progenitor cells); D: GFP+/CD45+/CD133+ (endothelial progenitor cells) in peripheral blood of the Saline 30 d and CCl₄ 30 d groups. No significant difference was detected between the groups by Student's *t* test.

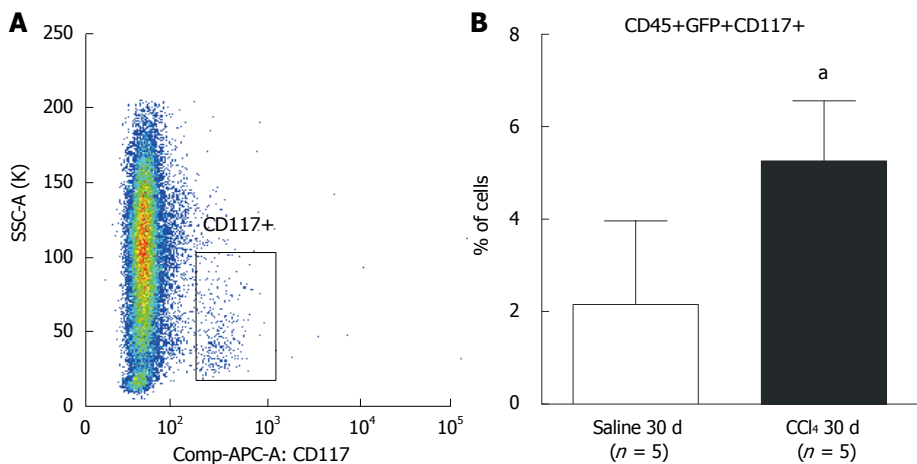


Figure 5 Flow cytometric analysis of subpopulations of CD117+ precursor cells in bone marrow of chimeric mice. A: Dot-plot analysis of CD117+ cells found in bone marrow. Side-bar dot-plots represent ancestry gating; B: A significantly greater population of CD117+ cells was observed in liver tissue from the CCl₄ 30 d group compared to the Saline 30 d group (30 d saline = 2.6 ± 1.3%; CCl₄ 30 d = 5.6 ± 1.8%) (²*P* = 0.0142). GFP: green fluorescent protein.

cular region, presenting fusiform morphology, rounded morphology and also very small nuclei (Figure 8B).

As we confirmed the increased migration of BM

GFP+ cells to the injured liver, we investigated if those cells were differentiating into activated HSCs and MF-like cells, which are responsible for the deposition of col-

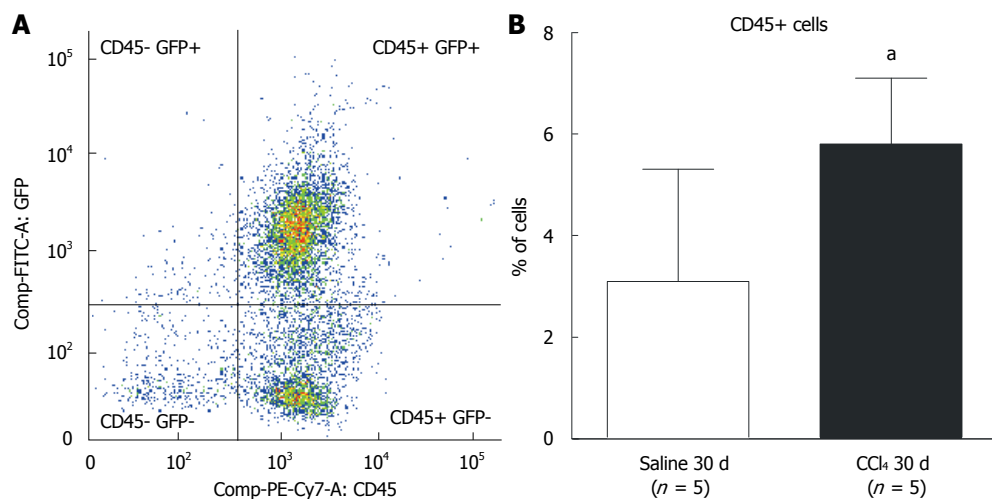


Figure 6 Flow cytometric analysis of bone marrow subpopulations in the liver of chimeric mice. A: Dot-plot analysis of cell populations in the liver; B: A significantly greater population of CD45+ cells was observed in liver tissue of animals from the CCl₄ 30 d group compared to the Saline 30 d group (30 d saline = 3.1% ± 2.2%; CCl₄ 30 d = 5.8% ± 1.3%) (^a*P* = 0.0458). GFP: green fluorescent protein.

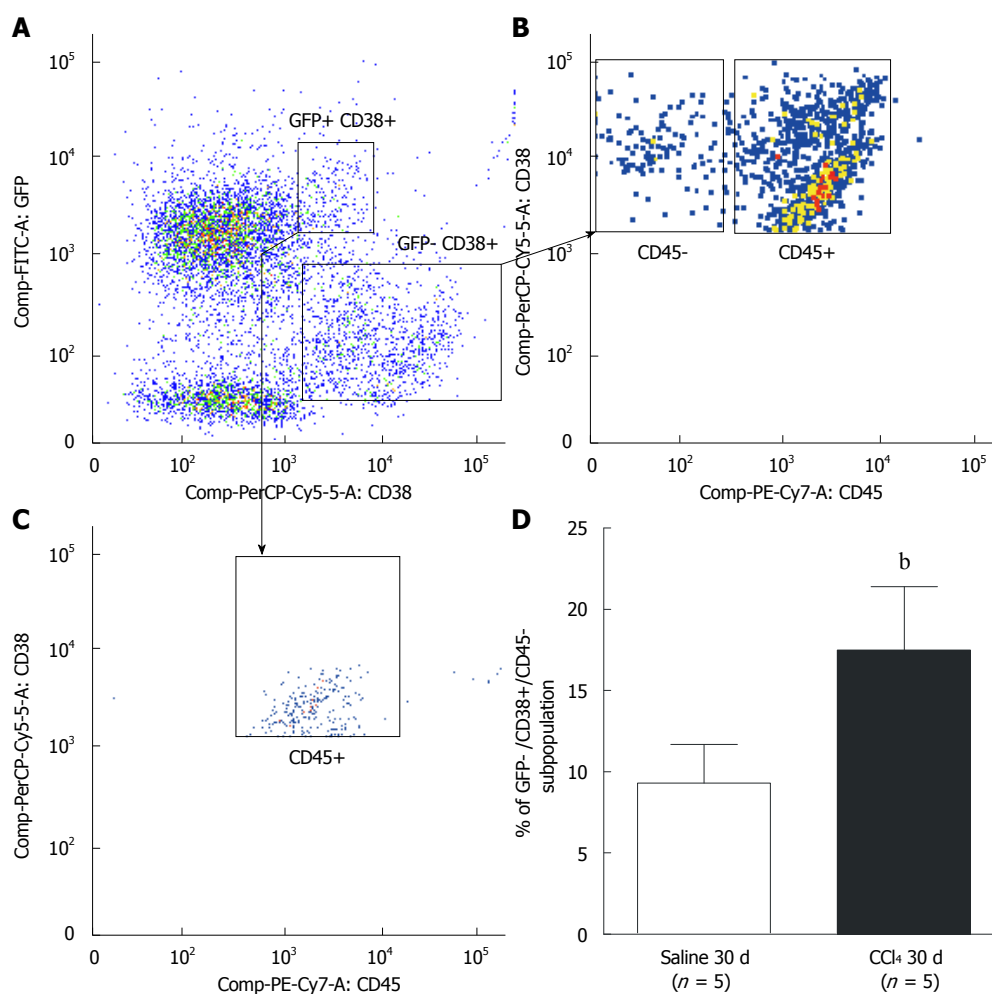


Figure 7 Representative analysis of CD38+ hepatic stellate cell subpopulations by flow cytometry. A: Two CD38+ subpopulations were observed: green fluorescent protein (GFP)+/CD38+ and GFP-/CD38+; B: Two subpopulations among GFP-/CD38+ cells were observed: GFP-/CD38+/CD45+ that identifies B lymphocytes, and GFP-/CD38+/CD45- that identifies hepatic stellate cells; C: Analysis of GFP+/CD38+ cells showed that all cells were of hematopoietic origin (CD45+); D: A significant increase of cells GFP-/CD38+/CD45- was observed in liver tissue of the CCl₄ 30 d group when compared to the Saline 30 d group (Saline 30 d = 9.3% ± 2.4%; CCl₄ 30 d = 17.5% ± 3.9%, ^b*P* = 0.004). The statistical test used was Student's *t* test.

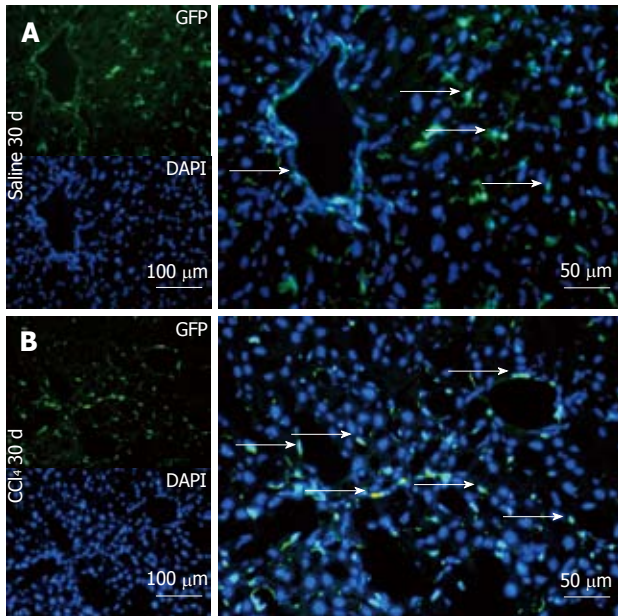


Figure 8 Representative direct fluorescence images of hepatic sections of chimeric animals after transplantation. Liver samples of chimeric animals after transplantation of green fluorescent protein (GFP)+ bone marrow mononuclear cell, chimeric animals that received saline (Saline 30 d) and chimeric animals that received CCl₄ (CCl₄ 30 d). In panel A (Saline 30 d), the GFP channel shows the presence of green fluorescence; in the 4, 6-diamino-2-phenylindole panel, nuclei are stained blue in the same field above; the merge panel superposes the two images, where GFP+ cells (arrows) can be seen distributed in major hepatic parenchyma and with fusiform morphology. In panel B (CCl₄ 30 d), GFP+ cells can be seen with greater distribution in the hepatic parenchyma, some fusiform morphology (white arrows) and others with rounded morphology. DAPI: 4,6-diamino-2-phenyl indole.

lagen, by using an α -SMA antibody as a specific marker for these cell types. Our results demonstrate that α -SMA+ cells in normal and irradiated/non-intoxicated livers are mainly distributed surrounding periportal regions (Figure 9A), while in intoxicated animals there is an increase of α -SMA+ cells that spread from periportal regions to parenchyma, representing initial septa formation (Figure 9B). These results indicate proliferation of cells with MF characteristics when there is liver damage. However, in our confocal analysis, we found no co-localization of α -SMA+ with GFP+ cells either in normal or injured tissue, suggesting that cells of BM origin do not contribute to the population of MFs, even after induction of liver injury.

DISCUSSION

In the present study, we showed that BM-derived progenitor subpopulations do not contribute to the fibrogenic MF population after liver injury in mice.

It is already known that the BM is altered after chronic hepatic disease^[27-29]. The presence of inflammatory cells in PB indirectly indicates alterations in the proliferation of cells in BM^[30]. We observed a significant increase in mature hematopoietic cells in the blood of CCl₄-intoxicated animals (Figure 3), indicating a chronic inflammatory condition 30 d after liver injury induction. Because inflamma-

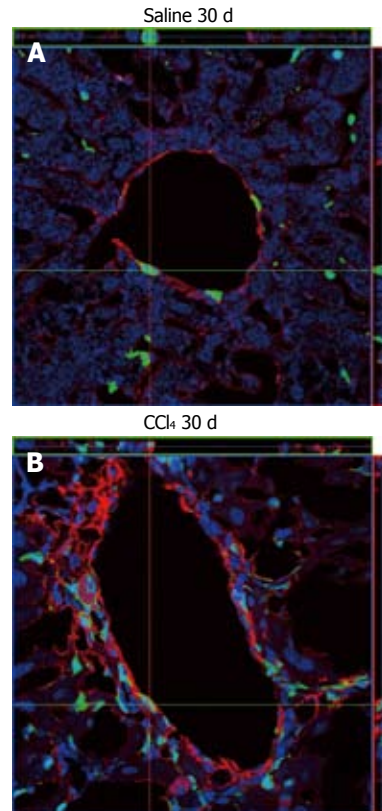


Figure 9 Immunostaining analysis of α -smooth muscle actin in liver samples from chimeric animals by confocal microscopy. A: α -smooth muscle actin (α -SMA)+ cells in the perivascular region were observed where green fluorescent protein (GFP)+ cells could also be seen, but the two cell types do not co-localize, as can be seen by the orientation of the red and green bars; B: An increase in reactivity against α -SMA around the perivascular region was observed, also with augmentation of GFP+ cells, but again these cell types do not co-localize. In both images the nuclei were stained with TO-PRO3 (blue).

tory cells are increased, it is expected that the progenitor compartment of BM should also be altered. In fact, we observed an increase in CD117 (c-Kit+) cells in BM of injured mice, which is a marker for BM progenitors such as common myeloid progenitors (CMPs)^[31].

Among the progenitor cells in blood, we could identify a GFP+/CD45+/CD34+ subpopulation, a rare population that is more related to hematopoietic progenitor cells^[32] but also to circulating fibrocytes^[19]. We found this GFP+/CD45+/CD34+ population at a very low percentage in total PB and it did not increase even after 30 d of liver injury. Because CMPs were increased in BM, we believe that hematopoietic stem cells are quickly stimulated to differentiate into CMPs in response to signaling from inflammatory cells at the injury site, thus giving primitive hematopoietic stem cells a short life-span. Consequently, recruitment of hematopoietic stem cells to blood may not be efficient. Endothelial progenitor cells (CD133+) may be affected by the same behavior. Concerning fibrocytes, Scholten *et al.*^[33] have shown that fibrocytes are stimulated to migrate even in non-injured liver in older but not in younger mice. Therefore, detection of fibrocytes in blood may be difficult since we used young mice. We tried to evaluate whether hematopoietic progenitors could be identified in the liver by flow cytometry.

Studies report that hematopoietic stem cells can comprise 0.1% to 1.0% of total blood cells as well as fibrocytes^[24]. Our samples presented a total hematopoietic cell frequency in liver of 6%, which is very low. For that reason, detection of rare cells in a low-frequency population is very difficult, and it will be necessary to have a

much larger sample to obtain reliable data to address this question. Although we could not detect if circulating fibroblasts were present in blood and liver samples, we suggest that this subpopulation did not contribute to liver fibrosis because no GFP+/ α -SMA+ cells were detected in our liver tissue specimens. Moreover, even if they did transdifferentiate to an MF-like cell, they would be present at such a low frequency that they would be unlikely to exert a major influence on fibrogenesis.

On the other hand, HSCs do contribute importantly to the fibrogenetic process^[34], but there is still controversy in the literature concerning the contribution of the BM to this liver subpopulation. Baba *et al.*^[35] reported co-localization of GFP and α -SMA in non-parenchymal cells in *in vitro* and *in vivo* models, whereas Higashiyama *et al.*^[36] showed a lack of co-localization of those markers after peak fibrosis. Our results corroborate the findings of Higashiyama *et al.*^[36], and suggest that BM-derived cells do not contribute to the HSC compartment. To confirm this hypothesis, we identified the HSCs by flow cytometry, using CD38 as a marker. The CD45-/CD38+ subpopulation was GFP negative, which agrees with our confocal microscopy results. Therefore, we suggest that the HSC population is not of BM hematopoietic origin, as it lacks both CD45 and GFP. Our results do not corroborate those reported by Miyata *et al.*^[9], who reported finding enhanced GFP+ HSCs in a longer injury induction experimental model, which may suggest that duration of injury could be a factor in determining the extent of BM cell contribution to fibrosis.

In conclusion, we found that BM progenitor cells do not contribute to fibrosis. However, there is a high response toward inflammatory cell recruitment that may contribute to fibrosis, by producing pro-inflammatory factors that stimulate HSCs and perivascular MFs of liver origin.

COMMENTS

Background

Bone marrow (BM) has been proposed as a source of cells for alternative therapy in liver diseases. Recent findings, however, suggest a potential deleterious effect of BM-derived cells in the regenerating liver.

Research frontiers

Results published so far show no consensus on the role of the BM in liver repair. Indeed, this issue remains one of the most controversial in the field of regenerative medicine. In this study, the authors demonstrate that BM stem cells do not participate in liver fibrogenesis.

Innovations and breakthroughs

Publications related to liver fibrosis and cell therapy have suggested that BM cells could contribute to liver fibrosis by differentiating into hepatic stellate cells (HSCs) and myofibroblasts (MFs), but have not identified which specific BM subpopulation participates in this process. In this study, the authors demonstrate that two BM subpopulations, the hematopoietic and endothelial progenitor cells, do not contribute to fibrosis by their differentiation to those fibrotic cells.

Applications

By understanding how BM cells function in an injured liver, this study is useful as a guide for strategies related to cell therapies using BM cells.

Terminology

Hematopoietic and endothelial progenitor cells are BM subpopulations which

participate in hematopoiesis and vasculogenesis, respectively. HSCs are non-parenchymal liver cells found in the perisinusoidal space (Space of Disse) and are pivotal in liver fibrogenesis by producing fibrillar extracellular matrix when in an activated state.

Peer review

In this study, the findings suggest that the response toward inflammatory cell recruitment by producing pro-inflammatory factors that stimulate HSCs and perivascular MFs of liver origin may contribute to fibrosis, while no evidence in the study supports that BM-derived progenitor cells contribute to the population of α -smooth muscle actin-producing cells.

REFERENCES

- 1 **Souza BS**, Nogueira RC, de Oliveira SA, de Freitas LA, Lyra LG, Ribeiro dos Santos R, Lyra AC, Soares MB. Current status of stem cell therapy for liver diseases. *Cell Transplant* 2009; **18**: 1261-1279
- 2 **Couto BG**, Goldenberg RC, da Fonseca LM, Thomas J, Gutfilen B, Resende CM, Azevedo F, Mercante DR, Torres AL, Coelho HS, Maiolino A, Alves AL, Dias JV, Moreira MC, Sampaio AL, Sousa MA, Kasai-Brunswick TH, Souza SA, Campos-de-Carvalho AC, Rezende GF. Bone marrow mononuclear cell therapy for patients with cirrhosis: a Phase 1 study. *Liver Int* 2011; **31**: 391-400
- 3 **Sakaida I**, Terai S, Yamamoto N, Aoyama K, Ishikawa T, Nishina H, Okita K. Transplantation of bone marrow cells reduces CCl4-induced liver fibrosis in mice. *Hepatology* 2004; **40**: 1304-1311
- 4 **Terai S**, Ishikawa T, Omori K, Aoyama K, Marumoto Y, Urata Y, Yokoyama Y, Uchida K, Yamasaki T, Fujii Y, Okita K, Sakaida I. Improved liver function in patients with liver cirrhosis after autologous bone marrow cell infusion therapy. *Stem Cells* 2006; **24**: 2292-2298
- 5 **Cao BQ**, Lin JZ, Zhong YS, Huang SB, Lin N, Tang ZF, Chen R, Xiang P, Xu RY. Contribution of mononuclear bone marrow cells to carbon tetrachloride-induced liver fibrosis in rats. *World J Gastroenterol* 2007; **13**: 1851-1854; discussion 1854-1856
- 6 **Oliveira SA**, Souza BS, Guimaraes-Ferreira CA, Barreto ES, Souza SC, Freitas LA, Ribeiro-Dos-Santos R, Soares MB. Therapy with bone marrow cells reduces liver alterations in mice chronically infected by *Schistosoma mansoni*. *World J Gastroenterol* 2008; **14**: 5842-5850
- 7 **Forbes SJ**, Russo FP, Rey V, Burra P, Ruge M, Wright NA, Alison MR. A significant proportion of myofibroblasts are of bone marrow origin in human liver fibrosis. *Gastroenterology* 2004; **126**: 955-963
- 8 **Shirakura K**, Masuda H, Kwon SM, Obi S, Ito R, Shizuno T, Kurihara Y, Mine T, Asahara T. Impaired function of bone marrow-derived endothelial progenitor cells in murine liver fibrosis. *Biosci Trends* 2011; **5**: 77-82
- 9 **Miyata E**, Masuya M, Yoshida S, Nakamura S, Kato K, Sugimoto Y, Shibasaki T, Yamamura K, Ohishi K, Nishii K, Ishikawa F, Shiku H, Katayama N. Hematopoietic origin of hepatic stellate cells in the adult liver. *Blood* 2008; **111**: 2427-2435
- 10 **Quintanilha LF**, Mannheimer EG, Carvalho AB, Paredes BD, Dias JV, Almeida AS, Gutfilen B, Barbosa da Fonseca LM, Resende CM, Rezende GF, Campos de Carvalho AC, Goldenberg RC. Bone marrow cell transplant does not prevent or reverse murine liver cirrhosis. *Cell Transplant* 2008; **17**: 943-953
- 11 **Mannheimer EG**, Quintanilha LF, Carvalho AB, Paredes BD, Gonçalves de Carvalho F, Takiya CM, Resende CM, Ferreira da Motta Rezende G, Campos de Carvalho AC, Schanaider A, dos Santos Goldenberg RC. Bone marrow cells obtained from cirrhotic rats do not improve function or reduce fibrosis in a chronic liver disease model. *Clin Transplant* 2011; **25**: 54-60
- 12 **Carvalho AB**, Quintanilha LF, Dias JV, Paredes BD,

- Mannheimer EG, Carvalho FG, Asensi KD, Gutfilen B, Fonseca LM, Resende CM, Rezende GF, Takiya CM, de Carvalho AC, Goldenberg RC. Bone marrow multipotent mesenchymal stromal cells do not reduce fibrosis or improve function in a rat model of severe chronic liver injury. *Stem Cells* 2008; **26**: 1307-1314
- 13 **Pinzani M**, Rombouts K. Liver fibrosis: from the bench to clinical targets. *Dig Liver Dis* 2004; **36**: 231-242
- 14 **Kisseleva T**, Brenner DA. Fibrogenesis of parenchymal organs. *Proc Am Thorac Soc* 2008; **5**: 338-342
- 15 **Hernandez-Gea V**, Friedman SL. Pathogenesis of liver fibrosis. *Annu Rev Pathol* 2011; **6**: 425-456
- 16 **Cassiman D**, Libbrecht L, Desmet V, Deneef C, Roskams T. Hepatic stellate cell/myofibroblast subpopulations in fibrotic human and rat livers. *J Hepatol* 2002; **36**: 200-209
- 17 **Benyon RC**, Arthur MJ. Extracellular matrix degradation and the role of hepatic stellate cells. *Semin Liver Dis* 2001; **21**: 373-384
- 18 **Parola M**, Marra F, Pinzani M. Myofibroblast-like cells and liver fibrogenesis: Emerging concepts in a rapidly moving scenario. *Mol Aspects Med* 2008; **29**: 58-66
- 19 **Bucala R**, Spiegel LA, Chesney J, Hogan M, Cerami A. Circulating fibrocytes define a new leukocyte subpopulation that mediates tissue repair. *Mol Med* 1994; **1**: 71-81
- 20 **Dolgachev VA**, Ullenbruch MR, Lukacs NW, Phan SH. Role of stem cell factor and bone marrow-derived fibroblasts in airway remodeling. *Am J Pathol* 2009; **174**: 390-400
- 21 **Haudek SB**, Xia Y, Huebener P, Lee JM, Carlson S, Crawford JR, Pilling D, Gomer RH, Trial J, Frangogiannis NG, Entman ML. Bone marrow-derived fibroblast precursors mediate ischemic cardiomyopathy in mice. *Proc Natl Acad Sci USA* 2006; **103**: 18284-18289
- 22 **Nimphius W**, Moll R, Olbert P, Ramaswamy A, Barth PJ. CD34+ fibrocytes in chronic cystitis and noninvasive and invasive urothelial carcinomas of the urinary bladder. *Virchows Arch* 2007; **450**: 179-185
- 23 **Kisseleva T**, Uchinami H, Feirt N, Quintana-Bustamante O, Segovia JC, Schwabe RF, Brenner DA. Bone marrow-derived fibrocytes participate in pathogenesis of liver fibrosis. *J Hepatol* 2006; **45**: 429-438
- 24 **Keeley EC**, Mehrad B, Strieter RM. The role of fibrocytes in fibrotic diseases of the lungs and heart. *Fibrogenesis Tissue Repair* 2011; **4**: 2
- 25 **Okabe M**, Ikawa M, Kominami K, Nakanishi T, Nishimune Y. 'Green mice' as a source of ubiquitous green cells. *FEBS Lett* 1997; **407**: 313-319
- 26 **March S**, Graupera M, Rosa Sarrias M, Lozano F, Pizcueta P, Bosch J, Engel P. Identification and functional characterization of the hepatic stellate cell CD38 cell surface molecule. *Am J Pathol* 2007; **170**: 176-187
- 27 **Meagher RC**, Sieber F, Spivak JL. Suppression of hematopoietic-progenitor-cell proliferation by ethanol and acetaldehyde. *N Engl J Med* 1982; **307**: 845-849
- 28 **Zhao S**, Fu YM, Li XF, Jin ZF, Zhao RB, Huang Q, Zhang FM, Zhang WH. Alterations of bone marrow sinusoidal endothelium in rat and patients with liver cirrhosis. *Dig Dis Sci* 2010; **55**: 654-661
- 29 **Dang SS**, Wang WJ, Gao N, Wang SD, Li M, Liu LY, Sun MZ, Dong T. Apoptotic bone marrow CD34+ cells in cirrhotic patients. *World J Gastroenterol* 2011; **17**: 2044-2048
- 30 **Bhunchet E**, Eishi Y, Wake K. Contribution of immune response to the hepatic fibrosis induced by porcine serum. *Hepatology* 1996; **23**: 811-817
- 31 **Franco CB**, Chen CC, Drukker M, Weissman IL, Galli SJ. Distinguishing mast cell and granulocyte differentiation at the single-cell level. *Cell Stem Cell* 2010; **6**: 361-368
- 32 **Kucia M**, Reza R, Jala VR, Dawn B, Ratajczak J, Ratajczak MZ. Bone marrow as a home of heterogeneous populations of nonhematopoietic stem cells. *Leukemia* 2005; **19**: 1118-1127
- 33 **Scholten D**, Reichart D, Paik YH, Lindert J, Bhattacharya J, Glass CK, Brenner DA, Kisseleva T. Migration of fibrocytes in fibrogenic liver injury. *Am J Pathol* 2011; **179**: 189-198
- 34 **Bataller R**, Brenner DA. Hepatic stellate cells as a target for the treatment of liver fibrosis. *Semin Liver Dis* 2001; **21**: 437-451
- 35 **Baba S**, Fujii H, Hirose T, Yasuchika K, Azuma H, Hoppo T, Naito M, Machimoto T, Ikai I. Commitment of bone marrow cells to hepatic stellate cells in mouse. *J Hepatol* 2004; **40**: 255-260
- 36 **Higashiyama R**, Inagaki Y, Hong YY, Kushida M, Nakao S, Niioka M, Watanabe T, Okano H, Matsuzaki Y, Shiota G, Okazaki I. Bone marrow-derived cells express matrix metalloproteinases and contribute to regression of liver fibrosis in mice. *Hepatology* 2007; **45**: 213-222

S- Editor Song XX L- Editor Webster JR E- Editor Yan JL